

DEFORMATION CHARACTERISTICS OF SLAG BASE-COURSE MATERIAL CONTAINING FLY ASH PELLET

Nobuyuki YOSHIDA¹ and Masaru NISHI²

¹ Member of JSCE, Ph.D., Associate Professor, Research Center for Urban Safety & Security, Kobe University (Rokkodai, Nada, Kobe 657-8501, Japan)

² Member of JSCE, Dr. Eng., Professor, Dept. of Civil Eng., Kobe University (Rokkodai, Nada, Kobe 657-8501, Japan)

This paper describes the deformation characteristics of a base-course material which is a mixture of steel-making slag, blast-furnace slag and fly ash pellet (here called 'the compound slag B'). The deformation characteristics are investigated by carrying out a repeated loading triaxial compression test: the equations expressing the resilient and permanent deformation behaviour are presented. It is shown that the compound slag B exhibits better deformation characteristics than Hydraulic mechanically stabilized slag (HMS), a standard slag base-course and that the same equations of representing the resilient and permanent deformation behaviour are applicable to the compound slag B as those for HMS and a previously-investigated compound slag.

Key Words : base-course, slag, fly ash, resilient deformation, permanent deformation, triaxial compression test, repeated loading, asphalt pavement

1. INTRODUCTION

Effective use of industrial by-product is essential to preservation of resources and decrease in energy consumption in Japan.

Slag is by-product in the iron and steel making process and has been increasingly used as base-course material. Hydraulic mechanically stabilized slag (hereafter called 'HMS'), is recognized as a standard slag base-course material in the design manual of asphalt pavements¹⁾, and it has been used in asphalt pavement practice. In the authors' laboratory, a compound slag has been investigated to encourage use of steel-making slag which was then little used as base-course material; it was a mixture of steel-making slag, gradually cooled blast-furnace slag and rapidly cooled blast-furnace slag in the ratio of 5: 3: 2 (hereafter called 'the compound slag A')^{2), 3), 4)}.

Most fly ash is by-produced at thermal power plants in Japan and the amount is expected to significantly increase in the near future. Fly ash is classified roughly into one from a combustion boiler of fine powdered coal (hereafter called 'fine powdered coal ash') and the other from a combustion boiler with fluidized bottom (hereafter called 'fluidized bottom ash'); the latter contains more lime and carbon components. Fly

ash pellet is made by solidifying these two types of fly ashes with cement and gypsum. It is then crushed and graded for use.

Deformation characteristics of base-course and subgrade in asphalt pavements are represented in terms of linear elastic constants in Japan. This is because of easiness of their use and determination in routine practice. However, much efforts have been made to express the deformation behaviour of base-course and subgrade in terms of non-linear elastic constants based upon laboratory repeated (or dynamic) loading tests especially in UK and USA, considering the fact that the conventional base-course and subgrade materials deforms nonlinearly even in a strain/stress level as small as encountered in actual pavements^{5), 6)}. Various equations representing the nonlinear deformation behaviour of base-course and subgrade have been proposed in the literature^{7), 8), 9)}.

In this study, investigated is another compound slag base-course material consisting of steel-making slag, blast-furnace slag and fly ash pellet mentioned above. Its deformation characteristics are investigated by carrying out repeated loading triaxial compression tests and discussed in comparison with those of the compound slag A and HMS.

Table 1 Components of compound slag B

Components	(%)
Steel-making slag	40
Blast-furnace slag	
gradually cooled	25
rapidly cooled	5
Fly ash pellet	30

Table 3 Constituents of fly ash pellet

Constituents	(%)
Powdered coal ash	65.2
Fluidized bottom ash	21.7
Desulfurized gypsum	4.4
Cement	8.7

Table 2 Physical properties of compound slag B components

Components	Specific gravity			Crushing strength (kN/pellet)
	surface-dried	absolutely-dried	apparently-dried	
Steel-making slag	3.39	3.34	3.47	1.8 - 7.2
Blast-furnace slag				
gradually cooled	2.46	2.38	2.65	1.0 - 3.2
rapidly cooled	2.65	2.59	2.74	-
Fly ash pellet	1.65	1.26	2.08	1.2 - 3.0

Table 4 Chemical components of fly ash

Constituents	Chemical components								
	SiO ₂	Al ₂ O ₃	MgO	T-CaO	f-CaO	f-C	Na ₂ O	K ₂ O	Others
Powdered coal ash	70.8	18.6	0.9	1.3	0.08	1.7	0.44	1.08	5.10
Fluidized bottom ash	27.2	14.1	0.6	13.4	3.6	26	0.34	0.61	14.15

2. RESILIENT AND PERMANENT DEFORMATION CHARACTERISTICS

(1) Repeated loading triaxial compression tests a) Test material and specimen preparation

Test material is a mixture of steel-making slag, blast-furnace slag and fly ash pellet as shown in **Table 1** (hereafter called 'the compound slag B'). **Table 2** shows some physical properties of the constituents. The fly ash pellet is a mixture of fine powdered coal ash, fluidized bottom ash, desulfurized gypsum and cement as given in **Table 3**. The chemical components of fine powdered coal fly ash and fluidized bottom ash are given in **Table 4**.

A preliminary study shows that the maximum

dry density of the compound slag B is 1.785 g/cm³ and the optimum water content is 17.8 %, that the maximum dry density is smaller and the optimum water content is larger than those of HMS and the compound slag A.

Test specimens are prepared as follows:

- 1) place the test material into a mould and compact it at the optimum water content;
- 2) detach the sample from the mould and cover it with plastic wraps and wet cloths;
- 3) cure it in the ground at a depth of 300mm for certain periods of time, 0, 0.5, 1, 3 and 6 months; and
- 4) trim the both ends of the sample to form a test specimen of 100mm in diameter and 200mm in height.

Table 5 Loading conditions

Loading time (s)	0.1
Pause time (s)	2.0
Number of load applications	20000
Applied stresses	
Mean principal stress (MPa)	Deviatoric stress (MPa)
0.078	0.147
	0.088
	0.059
	0.029
0.160	0.294
	0.206
	0.147
	0.088
	0.059
0.235	0.353
	0.235
	0.147
	0.088
	0.059

b) Test procedure

The testing apparatus used in this study is an ordinal repeated loading triaxial testing system with a dual cell for unsaturated soil specimens. Repeated axial loads are applied using a Bellofram cylinder connected with a dual-directional electromagnetic valve. The loading time is controlled by a timer. Repeated deviatoric loads are adjusted using a load cell between the piston and the Bellofram cylinder, a dynamic strain meter and a recorder. Friction between the loading piston and the outer cell is reduced by circulating fluid paraffin around the piston. Lubricated ends are formed using an annular plastic disk with silicon oil on each end of the specimen. The axial displacement is measured using a dial gauge connected with the loading piston and the volumetric change is measured using a pressure difference gauge or as readings of variation of water table in the inner cell.

A test specimen is first isotropically consolidated under the confining pressure applied in the subsequent repeated loading. Then, a prescribed deviatoric stress is applied repeatedly to the specimen with a loading time of 0.1s and a pause of 2s. The number of load applications is set as 20,000 at which the permanent axial strain increment usually becomes negligible. Subsequently, adjusting the confining pressure so as to keep the mean principle stress constant, the deviatoric stress is gradually reduced and applied

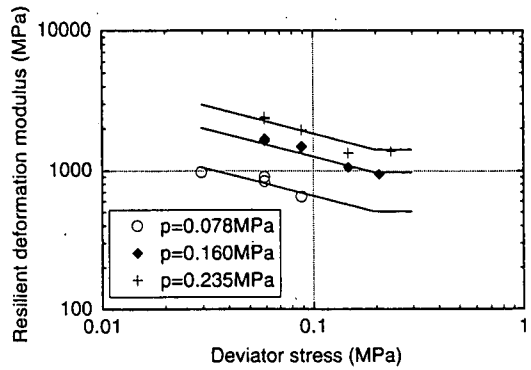


Fig. 1 Relationships between resilient deformation modulus and deviatoric stress (curing time = 3 months)

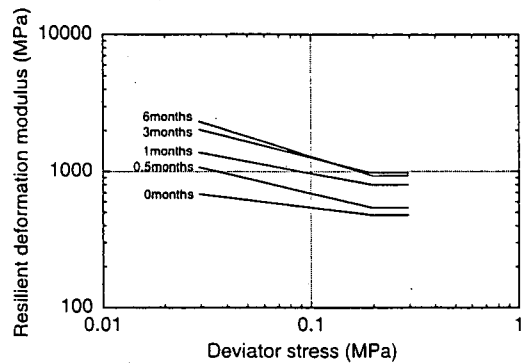


Fig. 2 Influence of curing time upon resilient deformation modulus (mean principal stress = 0.160 MPa)

to the specimen about 500 to 2,000 times to measure the resilient strain ¹⁰. All the tests are carried out under drained condition. The applied stress condition is summarized in **Table 5**. Note that fractions in the magnitude of applied stresses are due to unit conversion to SI.

(2) Deformation characteristics

a) Resilient deformation

The resilient deformation modulus, M_r , is calculated as a ratio of repeated deviatoric stress to resulting resilient axial strain. **Fig. 1** shows the relationships between resilient deformation modulus and deviatoric stress at a curing time of 3 months. Also shown in the figure are regression lines of which equation is presented later in this sub-section. It is seen that the resilient deformation modulus decreases as the deviatoric stress increases and that it, although not clear in this particular figure, tends to become constant at a deviatoric stress greater than about 0.196 MPa.

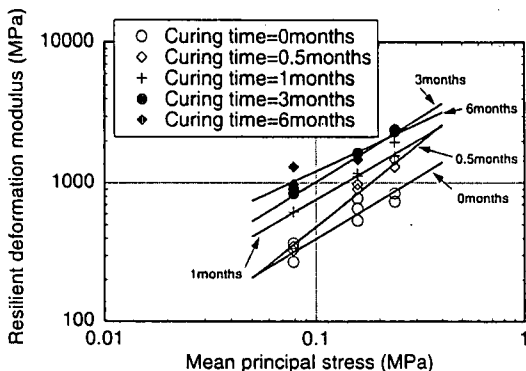


Fig. 3 Relationships between resilient deformation modulus and mean principal stress (deviatoric stress = 0.059 MPa)

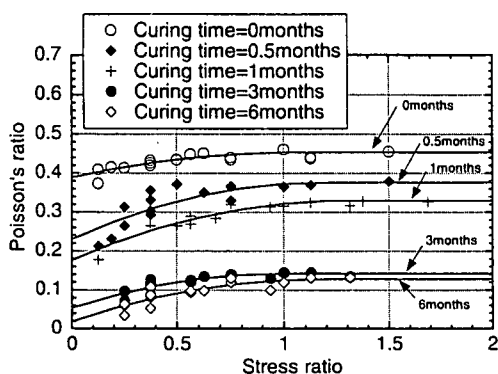


Fig. 4 Relationships between resilient Poisson's ratio and stress ratio

Table 6 Material constants for resilient deformation modulus

Curing time (months)	K	M	N
0	2622	0.918	0.187
0.5	5242	1.225	0.361
1	4077	0.803	0.288
3	5508	0.937	0.389
6	3443	0.705	0.482

Table 7 Material constants for resilient Poisson's ratio

Curing time (months)	A ₀	A ₁	A ₂
0	0.3900	0.119	-0.0556
0.5	0.2300	0.249	-0.1060
1	0.1770	0.237	-0.0917
3	0.2301	0.249	-0.1060
6	0.3896	0.120	-0.0556

This tendency was also observed in the test results on the compound slag A and HMS, and has been considered due to that, the material behaves like an clayey soil due to development of cementation effect similar to cohesion resulting from the hydraulic hardening nature inherent in these slag materials ^{3), 10), 11)}. On this ground, it is assumed, as shown later in this section, that the same form of a regression equation as for the compound slag A and HMS is applicable to this compound slag B. It is also seen that the greater the mean principal stress, the greater is the resilient deformation modulus.

Fig. 2 shows the influence of curing time upon the resilient deformation modulus in terms of regression lines at a mean principal stress of 0.160 MPa. It is seen that the resilient deformation modulus increases with curing time but that beyond 3months the increase seems slight.

Fig. 3 shows the relationships between resilient deformation modulus and mean principal stress at a deviatoric stress of 0.059 MPa. This figure confirms that the resilient deformation modulus increases with mean principal stress. Reduced influence of curing time upon the resilient deformation modulus can be seen after 3months.

The observations above are similar to those for HMS and the compound slag A tested in the past^{3), 10)} but the magnitude of the resilient deformation modulus of the compound slag B is slightly greater than that of HMS and a bit smaller than that of the compound slag A. The form of the regression equation representing the resilient deformation modulus is the same as that for HMS and the compound slag A; it is expressed, in terms of deviatoric stress and mean principal stress, as follows:

$$M_r = K p^M (0.196/q)^N \quad (1)$$

where M_r is resilient deformation modulus in MPa, and p and q are mean principal stress ($= (\sigma_1 + 2\sigma_3)/3$) and deviatoric stress ($= \sigma_1 - \sigma_3$) in MPa, respectively. K , M and N are material constants of which values are given in Table 6. Note that N is zero for $q \geq 0.196$ MPa.

Fig. 4 shows the resilient Poisson's ratio in terms of stress ratio ($= q/p$). It is seen that as the stress ratio increases, the Poisson's ratio increases and that the Poisson's ratio decreases as the curing time increases. Similar observation was also obtained for HMS and the compound slag A ³⁾. The regression equation is expressed as

$$v_r = A_0 + A_1 \eta + A_2 \eta^2 \quad (2)$$

Table 8 Material constants for permanent axial strain

Curing time (months)	p (MPa)	q (MPa)	a	b	ϵ_{p0} ($\times 10^{-3}$)	$\epsilon_{p,ult}$ ($\times 10^{-3}$)	
0	0.235	0.353	15973	5.0669	0.725	0.922	
		0.147	14226	4.3851	0.265	0.493	
		0.088	16644	15.025	0.230	0.297	
	0.157	0.294	8299	2.3966	1.540	1.957	
		0.147	23109	3.6289	0.360	0.636	
		0.088	13189	7.0558	0.395	0.537	
	0.078	0.147	8627.2	3.1038	1.225	1.577	
		0.088	6901.8	2.5258	0.760	1.156	
		0.059	80930	14.279	0.265	0.335	
	0.5	0.235	0.353	13776	2.9961	0.490	0.824
			0.147	157905	8.2886	0.270	0.391
			0.088	13797	9.5055	0.175	0.280
0.157		0.294	11138	3.9115	0.635	0.891	
		0.147	9963.9	9.0869	0.275	0.385	
		0.088	33295	8.7180	0.165	0.280	
0.078		0.147	9094.4	3.3853	0.510	0.805	
		0.088	7719.9	11.867	0.255	0.339	
		0.059	480.93	28.531	0.205	0.240	
1	0.235	0.353	18301	4.9479	0.335	0.537	
		0.147	23910	18.766	0.130	0.183	
		0.088	8087.6	11.876	0.055	0.139	
	0.157	0.294	1912.8	16.507	0.510	0.571	
		0.147	15613	8.0019	0.310	0.435	
		0.088	18809	23.525	0.110	0.153	
	0.078	0.147	66926	4.4630	0.205	0.429	
		0.088	12322	9.1026	0.200	0.310	
		0.059	42215	11.651	0.100	0.186	
3	0.235	0.353	39652	9.7680	0.130	0.232	
		0.147	26743	15.158	0.125	0.191	
		0.088	133650	23.420	0.045	0.088	
	0.157	0.294	17363	6.0783	0.235	0.400	
		0.147	15530	11.327	0.135	0.223	
		0.088	28659	17.839	0.105	0.161	
	0.078	0.147	32904	19.732	0.185	0.236	
		0.088	103509	26.225	0.095	0.157	
		0.059	44640	16.772	0.075	0.135	
6	0.235	0.353	35715	14.037	0.090	0.161	
		0.147	30199	22.612	0.085	0.129	
		0.088	20199	198.28	0.040	0.045	
	0.157	0.294	27860	19.048	0.110	0.162	
		0.147	23456	13.675	0.090	0.163	
		0.088	11201	39.060	0.075	0.101	
	0.078	0.147	74310	9.4394	0.075	0.181	
		0.088	48392	14.352	0.045	0.115	
		0.059	49312	16.157	0.050	0.112	

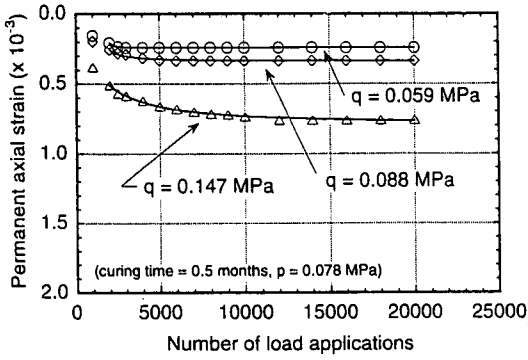


Fig. 5 Relationships between permanent axial strain and number of load applications

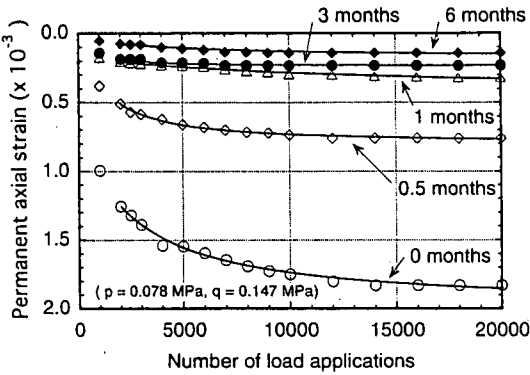


Fig. 6 Influence of curing time upon development of permanent axial strain

where η is stress ratio and A_0 , A_1 and A_2 are material constants of which values are given in **Table 7**.

b) Permanent deformation

Fig. 5 shows the relationship between the permanent axial strain and the number of load applications for the curing time of 0.5 months and the applied mean principal stress of 0.078 MPa. Also shown in the figure are the regression curves of which equations are given below. It is observed that the permanent axial strain increases with the number of load applications rapidly at the beginning, then gradually at the number of load applications greater than about 2000. It is also seen that the larger the applied stress, the larger is the magnitude of the resulting permanent axial strain.

Fig. 6 illustrates the influence of curing time upon the development of permanent axial strain for the mean principal stress of 0.078 MPa and the deviatoric stress of 0.147 MPa. As can be seen, the longer the curing time, the smaller the magnitude of the permanent axial strain is.

Similar tendencies have been also observed in

the test results on the compound slag A and HMS; however, the magnitude of the resulting permanent axial strain appears to be larger than the compound slag A and smaller than HMS.

The regression equation is given as

$$\epsilon_p = \epsilon_{p0} + (N - N_0) / \{ (a + b(N - N_0)) \} \quad (3)$$

where N is the number of load applications, N_0 is the reference number of load applications (= 2000), ϵ_p is permanent axial strain at N , ϵ_{p0} is permanent axial strain at N_0 , and a and b are experimental constants. Note that ϵ_{p0} and the parameters a and b are obtained for each combination of curing time, applied deviatoric stress and applied mean principal stress, as given in **Table 8**.

Table 9 Material constants for ultimate permanent axial strain

Curing time (months)	k (x 10 ⁻³)	u	v
0	0.894	1.100	1.029
0.5	1.264	0.947	0.432
1	0.550	0.714	1.015
3	0.353	0.423	0.724
6	0.137	0.604	0.645

Using Equ. (3), the ultimate permanent axial strain $\epsilon_{p,ult}$ is then computed by setting N as infinity in the above equation, and its relationship with deviatoric stress and mean principal stress is represented by

$$\epsilon_{p,ult} = k q^u / p^v \quad (4)$$

where $\epsilon_{p,ult}$ is ultimate permanent axial strain, and k , u and v are experimental constants. The experimental constants k , u and v are obtained for each curing time as given in **Table 9**.

3. CONCLUSIONS

The following conclusions can be drawn from this study.

- 1) The resilient deformation modulus of the compound slag B decreases as the deviatoric stress increases and tends to become constant at a deviatoric stress greater than about 0.196 MPa. It increases with mean principal stress and also with curing time. It is indicative that cementation effect develops due to the hydraulic hardening nature inherent in these slag materials.
- 2) The Poisson's ratio of the compound slag B increases as the stress ratio increases, and it decreases as the curing time increases.
- 3) The permanent axial strain of the compound slag B increases with the number of load applications rapidly at the beginning, then gradually at the number of load applications greater than about 2000. The larger the applied stress, the larger is the magnitude of the resulting permanent axial strain.

- 4) The compound slag B exhibits deformation characteristics equivalent to or better than HMS, a standard slag base-course material, and a bit worse than the compound slag A.

REFERENCES

- 1) Japan Road Association: *Design manual of asphalt pavements in Japan*, 1992. (in Japanese)
- 2) Nishi, M. and Kawabata, K.: Some basic and mechanical properties of iron and steel slags as base-course materials, *Proc. of JSCE*, No.414/V-12, pp. 89-98, 1990. (in Japanese)
- 3) Nishi, M., Yoshida, N., Tsujimoto, T. and Hatakeyama, S.: Deformation characteristics of iron and steel slags and crushed stone as base-course materials, *Proc. Int. Symp. Pre-Failure Deform. Char. Geomaterials*, Sapporo, Vol. 1, pp. 287-292, 1994.
- 4) Nishi, M., Kawabata, K. and Yoshida, N.: Behaviour of asphalt pavements in circular road tests and its analysis with special emphasis on slag base-courses, *Memoirs of Faculty of Engng.*, Kobe Univ., No. 37, pp. 1-23, 1990.
- 5) Hicks, R.G. and Monismith, C.L.: Factors influencing the resilient response of granular materials, *Highway Research Record*, No. 345, pp. 15-31, 1971.
- 6) Brown, S.F.: Repeated load testing on a granular material, *Jour. of Geotech. Engng. Div.*, ASCE, Vol. 100, No. C7, pp. 825-841, 1974.
- 7) Brown, S.F., Lashine, A.K.F. and Hyde, A.F.L.: Repeated load triaxial testing of a silty clay, *Geotechnique*, Vol. 25, No. 1, pp. 95-114, 1975.
- 8) Uzan, J., Witzczak, M.W., Scullion, T. and Lytton, R.L.: Development and Validation of realistic pavement response models, *Proc., 7th Inter. Conf. on Asphalt Pavements*, pp. 334-350, 1992.
- 9) Pappin, J.W., Brown, S.F. and O'Reilly, M.P.: Effective stress behaviour of saturated and partially saturated granular material subjected to repeated loading, *Geotechnique*, Vol. 42, No. 3, pp. 485-497, 1992.
- 10) Nishi, M.: Mechanics of flexible pavements, *A seminar text*, Kansai Branch of JSCE, pp. 1-34, 1979. (in Japanese)
- 11) Yoshida, N., Sano, M., Hirotsu, E., Nishi, M., Arai, T. and Tohyama, S.: Performance and layer equivalency factors of compound slag mixed with fly ash pellet, *Jour. of Pavement Engng.*, JSCE, Vol. 3, pp. 147-156, 1998. (in Japanese)

(Received May 10, 1999)

フライアッシュペレットを混合したスラグ路盤材の変形特性

吉田信之・西 勝

石炭灰を排煙脱硫石膏とセメントで固化し粉碎・粒度調整したもの(フライアッシュペレット)、製鋼スラグ、高炉スラグを混合した複合スラグ路盤材料(複合スラグBと称する)の復元及び残留変形特性を、室内繰返し三軸圧縮試験によって調べた。その結果、1)複合スラグBの復元変形係数は、軸差応力の増加とともに減少し一定値に収束し、また平均主応力の増加とともに増加すること、2)復元ポアソン比は、応力比の増加とともに増加すること、3)残留軸ひずみは、繰返し載荷回数とともに増加するが、特に載荷初期に急増しその後漸増すること等が明らかになった。さらに、従来の複合スラグよりは劣るものの、標準的な水硬性粒度調整高炉スラグ(HMS)よりは優れた変形特性であることが示唆されている。